

## Studying the normal-fluid flow in Helium-II using metastable helium molecules

W. Guo · J.D. Wright · S.B. Cahn · J.A. Nikkel · D.N. McKinsey

Received: date / Accepted: date

**Abstract** We demonstrate that metastable helium molecules can be used as tracers to visualize the flow of the normal fluid in superfluid  $^4\text{He}$  using a laser-induced-fluorescence technique. The flow pattern of a normal-fluid jet impinging on the center of a copper disc is imaged. A ring-shaped circulation structure of the normal fluid is observed as the jet passes across the disc surface. The fluorescence signal for the molecules trapped in the circulation structure is measured as a function of time after we turn off the molecule source. The radiative lifetime and density of the molecules can be determined by fitting the measured data using a simple analytic model. We also discuss a proposed experiment on using a previously developed molecule tagging-imaging technique to visualize the normal-fluid velocity profile during the transition of quantum turbulence in a thermal counterflow channel.

**Keywords** Visualization · Helium molecule · Jet impingement · Quantum turbulence

**PACS** 47.27.-i · 29.40.Gx · 67.25.dk · 67.25.D-

### 1 Introduction

Recently, particle image velocimetry with polymer micro-spheres and hydrogen isotopes has been used to study liquid helium flows [1,2] and solid hydrogen tracers have been used to visualize the quantized vortices [3,4]. However, the dynamics of micron-sized tracers in the presence of vortices are complex [1]. One must account for particle-vortex interactions [5] in order to extract an accurate measurement of the local normal-fluid velocity. Another approach to image the flow in liquid helium is neutron absorption tomography [6], which uses  $^3\text{He}$  as a neutral tracer and requires a finely collimated neutron beam and the ability to raster the neutron beam through the region of interest. Here we shall demonstrate that metastable  $\text{He}_2^*$  triplet molecules as neutral tracers can

---

W. Guo · J.D. Wright · S.B. Cahn · J.A. Nikkel · D.N. McKinsey  
Physics Department, Yale University,  
New Haven, CT 06520, USA  
Tel.: 203-432-3825  
Fax: 203-432-9710  
E-mail: wei.guo@yale.edu

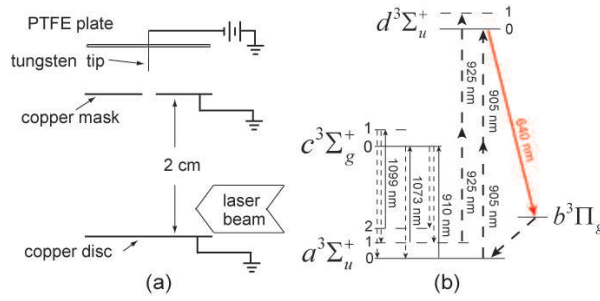


**Fig. 1** (Color online) (a) Schematic diagram showing the experimental setup. (b) Schematic diagram showing the cycling transitions for imaging the  $\text{He}_2^*$  triplet molecules.

be a powerful tool for helium hydrodynamic research. Metastable  $\text{He}_2^*$  molecules can be imaged using a laser-induced-fluorescence technique which involves only table-top laser systems [7,8].  $\text{He}_2^*$  molecules follow the motion of the normal fluid without being affected by vortices at temperatures above 1 K [9] due to their small effective mass in liquid  $^4\text{He}$  [10], hence they are ideal tracers for the normal fluid. In the following demonstration experiment, the real time dynamics of a normal-fluid jet impinging on the center of a copper disc is studied by using the molecule visualization technique.

## 2 Experiment and results

The schematic diagram of the experimental setup is shown in Fig. 1 (a). A sharp tungsten tip was mounted at the center of a polytetrafluoroethene (PTFE) plate. A grounded copper disc 2 cm in diameter and 0.5 mm thick was placed about 3 mm away from the tip apex as a mask. A hole 1 mm in diameter was cut at the center of the copper mask. A second grounded copper disc with no hole cut at its center was placed 2 cm below the copper mask. The whole device was held at the center of a  $250 \text{ cm}^3$  helium cell and was thermally linked to a helium bath. The temperature of the system was controlled to be at about 2 K by directly pumping on the helium bath.

To produce  $\text{He}_2^*$  molecules in the liquid helium, a negative voltage of amplitude higher than the field-emission threshold is applied to the tip [11,12]. Electrons emitted by the tungsten tip move from the tip region to the copper mask plate under the applied electric field. The moving electrons continuously pull the normal fluid and lead to the formation of a normal-fluid jet [12]. Associated with the emitted electrons,  $\text{He}_2^*$  molecules in both spin singlet and triplet states are produced near the tip apex. The singlet molecules radiatively decay in a few nanoseconds [13], while the triplet molecules are metastable with a radiative lifetime of about 13 s in liquid  $^4\text{He}$  [14]. At 2.0 K, a  $\text{He}_2^*$  molecule diffuses less than 1 mm during its lifetime [7]. The generated metastable  $\text{He}_2^*$  molecules are essentially entrained in the normal-fluid jet. As the jet reaches the surface of the mask plate, part of it can pass through the hole and keep on flowing to the bottom copper disc. Since both the mask and bottom disc were grounded in the experiment, few electrons could leak through the small hole in the mask. Hence, in the region between the mask and the bottom disc, the normal fluid moves without any electron pulling force on it, and its genuine hydrodynamic motion can be visualized by imaging the metastable  $\text{He}_2^*$  molecules entrained.

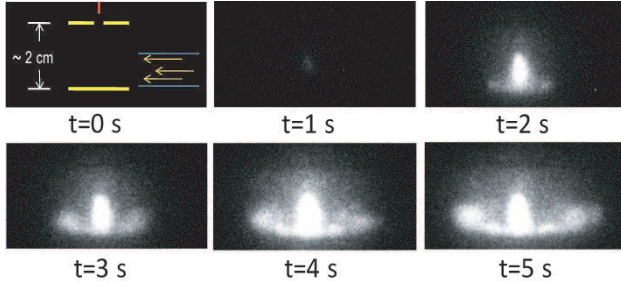


**Fig. 2** (Color online) The motion of a normal-fluid jet impinging on the center of a copper disc. The images were taken at 0 to 5 s after a -800 V voltage was applied to the tungsten tip.

To image the  $\text{He}_2^*$  molecules in the triplet state, a single pulsed laser at 905 nm is used to drive the molecules out of the  $a^3\Sigma_u^+$  state to produce 640 nm fluorescent light through a cycling transition (see Fig. 1 (b)) [8]. However, during the cycling transition,  $\text{He}_2^*$  molecules may fall to the long-lived excited vibrational levels of the  $a^3\Sigma_u^+$  state and are lost for subsequent cycles [8, 15]. To recover the lost molecules, we use continuous fiber lasers at 1073 nm and 1099 nm to repump the molecules from the  $a(1)$  to the  $c(0)$  state and from the  $a(2)$  to the  $c(1)$  state, respectively. Molecules in the  $c$  states have a chance to decay back to the  $a(0)$  state and can be used again. In the experiment, the intensities of the fiber lasers at 1073 nm and 1099 nm were chosen to be  $3 \text{ W/cm}^2$  and  $1.5 \text{ W/cm}^2$ , respectively. The intensity of the pulsed laser at 905 nm was  $500 \mu\text{J/cm}^2$  per pulse, and the repetition rate was 500 Hz. The pulsed laser beam was overlapped with the continuous laser beams in the region near the bottom disc and both were expanded to a spot size of  $1 \text{ cm}^2$ . All the laser beams pass through a pair of anti-reflection coated windows on the cell with negligible heating inside the cell.

A typical set of images showing the motion of a normal impinging normal-fluid jet on the center of the bottom disc is shown in Fig. 2. These images were taken with an intensified CCD camera successively from 0 s to 5 s at one second time intervals after a -800 V voltage was applied to the tip. The camera was synchronized to each laser pulse and exposed for  $6 \mu\text{s}$  so as to minimize dark current. The number of camera exposures for each image was chosen to be 50. As one can see, the normal-fluid jet enters the laser illumination region at  $t=1 \text{ s}$  and a weak signal due to the jet front can be seen. The jet then impinges on the bottom disc with a velocity of about  $1 \text{ cm/s}$  and leads to a radial wall jet [16] on the disc surface. As the radial wall jet passes the edge of the bottom disc, a ring-shaped circulation structure of the normal fluid appears near the periphery of the bottom disc. In our experiment, only the part of the vortex ring that was illuminated by the laser beams was visible. Hence the bright round regions near the edge of the bottom disc in the later images represent the cross-section view of the vortex ring. The impingement of a free circular jet onto a flat surface at normal incidence is of interest in many practical problems, such as jet blast, airplane vertical takeoff and landing, and particularly atmospheric microbursts [17] which is an event where a mass of cool dense air falls to the ground and spreads horizontally and radially from the impingement site, often creating hurricane-force winds. In our experiment, the impinging velocity of the jet can be controlled easily by varying the electric current. We even developed a technique for measuring the local flow velocity along the jet by tagging a small group of  $\text{He}_2^*$  molecules using a focused 910 nm pump laser pulse and

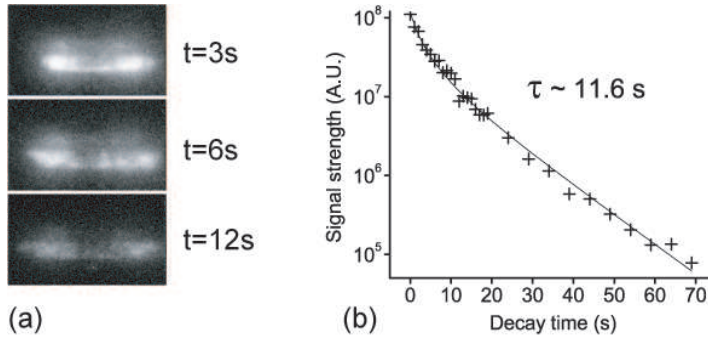


**Fig. 3** (a) Fluorescence images showing the He<sub>2</sub>\* molecules trapped in the normal-fluid circulation structure at 3 s, 6 s and 12 s after the tip was turned off. (b) The collected fluorescence light in arbitrary unit as a function of time after the tip was turned off. The crosses represent the measured data. The solid line is a least-squares fit to the measured data using the formula as discussed in the text.

imaging only the tagged molecules at a delayed time using an expanded 925 nm probe laser pulse. The pump laser drives the molecules from the  $a(0)$  state to the  $c(0)$  state where part of the molecules decay to the  $a(1)$  state (see Fig. 1 (b)). The probe laser then drives the  $a(1)$  molecules to the  $d$  state to produce the fluorescent light [18]. Our simple but convenient setup combined with the molecule detection technique may provide a new way to simulate and understand phenomena in a jet impinging process. A detailed study on jet impingement may be conducted in the future.

As we turn off the voltage on the tungsten tip, the source of the normal-fluid jet is off immediately, but the ring-shaped circulation on the periphery of the bottom disc can last for a few more seconds. Typical images taken with the same 905 nm laser settings but at 3 s, 6 s and 12 s after the tip was turned off are shown in Fig. 3 (a). The central bright feature with respect to Fig. 2 is absent since the jet is turned off. The He<sub>2</sub>\* molecules initially trapped in the core region of the circulation structure can stay there for long time even after the circulation dies away since there was no net normal-fluid flow to disperse the molecules. The fluorescence signal decreases gradually as the molecules decay with time. This indeed provides us a convenient way to study the decay process of the He<sub>2</sub>\* molecules. The crosses in Fig. 3 (b) represent the measured total fluorescence light in arbitrary unit as a function of the decay time. The decay process of the He<sub>2</sub>\* molecules in the experiment can be simply described by the following equation

$$\frac{dn}{dt} = -\frac{n}{\tau} - \alpha \cdot n^2 \quad (1)$$

where  $n$  is the molecule density,  $\tau$  is the molecule radiative decay lifetime and  $\alpha$  is the bimolecular Penning ionization decay coefficient [19]. The solution for Eq. (1) is

$$n(t) = n_0 \cdot \frac{e^{-t/\tau}}{1 + n_0 \alpha \tau (1 - e^{-t/\tau})} \quad (2)$$

where  $n_0$  is the initial molecule density. The fluorescence signal  $I(t)$  as a function of time can be written as

$$I(t) = I_0 \cdot \frac{e^{-t/\tau}}{1 + n_0 \alpha \tau (1 - e^{-t/\tau})} \quad (3)$$

where  $I_0$  is the initial fluorescence signal strength. The solid line in Fig. 3 (b) is a least-squares fit to the measured data based on Eq. (3). The obtained molecule radiative lifetime  $\tau$  is 11.6 s which is close to the previously measured one [14]. As one can see in Fig. 3 (b), the decay curve bends and deviates from the straight line  $e^{-t/\tau}$  decay at beginning. This is because that initially the molecule density is high and the Penning ionization decay dominates the decay process. The fitted value for quantity  $n_0\alpha$  is  $0.35 \text{ s}^{-1}$ . If we take  $\alpha$  to be  $2.5 \times 10^{-10} \text{ cm}^3 \text{ s}^{-1}$  at 2 K [19], the initial molecule density  $n_0$  is estimated to be  $1.4 \times 10^9 \text{ cm}^{-3}$ .

### 3 Proposal on visualizing the normal-fluid velocity profile in a channel

The ability to trace the normal-fluid flow and quantitatively measure the normal-fluid velocity provides for us the chance to better understand the role of the normal fluid in many hydrodynamical processes of superfluid helium. For example, it has been known for many years that in a counterflow channel with small aspect ratio there exist two different states of quantum turbulence of Helium II denoted by Tough as T-1 and T-2 states [20]. The T-1 state appears at low values of heat flux while the T-2 state appears at higher heat flux and is characterized by a much higher vortex line density. Melotte and Barenghi studied the nature of the two turbulent states and proposed that this puzzle was related to the stability of the normal fluid [21]. In the T-1 state, the superfluid is turbulent, but the vortex line density is not sufficient to significantly alter the laminar Poiseuille-like profile of the normal fluid. As the heat flux is increased, eventually the line density becomes large enough to destabilize the normal fluid and the normal-fluid flow becomes turbulent in the T-2 state.

So far, there is no direct experimental result to confirm Melotte and Barenghi's idea. We propose that by using the molecule tagging-imaging technique [18], we shall be able to provide useful experimental information. As shown in Fig. 4, we may use a strong beta source [8] (or field emitter [18]) to continuously produce high density  $\text{He}_2^*$  molecules in a counterflow channel. A focused 910 nm pump laser pulse prepares a straight line of tagged molecules. At an appropriate delay time, an expanded 925 nm probe laser pulse can then be used to show the shape of the tagged-molecule line. When the normal fluid is in laminar flow, a straight molecule line should deform to a parabolic curve due to the Poiseuille-like velocity profile of the normal fluid in the channel. While when the normal fluid is in the turbulent state, a nearly straight broadened molecule line should be expected due to the flat, turbulent uniform normal-fluid velocity profile across most of the channel [22]. As a result, we should be able to determine the normal-fluid velocity profile in the channel, hence distinguishing between the laminar flow and the turbulent flow states of the normal fluid. The vortex line density needs to be measured and one will know if the T-1 to T-2 transition of quantum turbulence is indeed coincident with the turbulent transition of the normal fluid as suggested by Melotte and Barenghi.

### 4 Conclusions

In conclusion, we have demonstrated that metastable  $\text{He}_2^*$  molecules can be used as tracers to study the dynamics of the normal fluid in superfluid  $^4\text{He}$ . The previously developed techniques for measuring the velocity of the normal fluid enable us to further

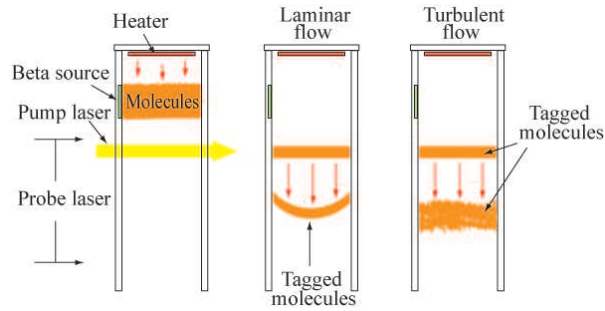


**Fig. 4** (Color online) Schematic diagram showing the proposed experiment on imaging the normal-fluid velocity profile in a counterflow channel using the molecule-tagging technique as discussed in the text.

explore many interesting problems such as jet impingement and the two stages of quantum turbulence in a thermal counter flow channel.

**Acknowledgements** We would like to thank Prof. Joe Vinen for helpful discussions.

## References

1. T. Zhang and S.W. Van Sciver, *J. Low Temp. Phys.* **138**, 865 (2005).
2. T. Zhang and S.W. Van Sciver, *Nat. Phys.* **1**, 36 (2005).
3. G.P. Bewley, *et al.*, *Nature* **441**, 588 (2006).
4. M.S. Paoletti, *et al.*, *Phys. Rev. Lett.* **101**, 154501 (2008).
5. D. Kivotides, *Phys. Rev.* **B78**, 224501 (2008).
6. M.E. Hayden, *et al.*, *Phys. Rev. Lett.* **93**, 105302 (2004).
7. D.N. McKinsey, *et al.*, *Phys. Rev. Lett.* **95**, 111101 (2005).
8. W.G. Rellergert, *et al.*, *Phys. Rev. Lett.* **100**, 025301 (2008).
9. W.F. Vinen, in *Low Temperature Physics*, AIP Conf. Proc. No. **850** (AIP, New York, 2006), p. 169.
10. A.V. Benderskii, *et al.*, *J. Chem. Phys.* **117**, 1201 (2002).
11. P.V.E. McClintock, *et al.*, *Cryogenics* **13**, 556 (1973).
12. R. Mehrotra, *et al.*, *J. Low Temp. Phys.* **36**, 47 (1979).
13. C.F. Chabalowski *et al.*, *J. Chem. Phys.* **90**, 2504 (1989).
14. D.N. McKinsey, *et al.*, *Phys. Rev.* **A59**, 200 (1999).
15. W.G. Rellergert, Ph.D. thesis, Yale University, 2008.
16. M.B. Glauert, *J. Fluid Mech. Vol. 1*, 625 (1956).
17. T.T. Fujita, SMRP Research Paper **210**, 122 pp (1985).
18. W. Guo, *et al.*, *Phys. Rev. Lett.* **102**, 235301 (2009).
19. J.W. Keto *et al.*, *Phys. Rev.* **A10**, 887 (1974).
20. J.T. Tough, in *Progress in Low Temperature Physics*, Superfluid Turbulence Vol. VIII (North-Holland, Amsterdam, 1982).
21. D.J. Melotte and C.F. Barenghi, *Phys. Rev. Lett.* **80**, 4181 (1998).
22. L.D. Landau and E.M. Lifshitz, *Fluid Mechanics*, (Butterworth-Heinemann, New York, 1987) 2nd edition.